Confined Doping LMA Fibers for High Power Single Frequency Lasers

Matthew A Cooper[a,*], Stefan Gausmann[a], Jose E. Antonio Lopez[a], Axel Schülzgen[a], and Rodrigo Amezcua Correa[a]

[a]University of Central Florida, CREOL, 4304 Scorpius St, Orlando, FL 32816

ABSTRACT

Fiber laser systems with high average power, narrow linewidth, and nearly diffraction limited beam quality are desirable for applications in areas such as gravitation wave detection or directed energy. In particular, these systems have special fiber design requirements and finding the right balance between large mode areas to mitigate unwanted nonlinear effects such as Stimulated Brillouin Scattering (SBS) while maintaining fundamental mode operation is a challenging task. A promising approach to achieve this goal relies on confining the rare earth dopant to the central region of the central LMA core and therefore providing preferential gain to the fundamental mode while simultaneously minimizing the spatial overlap of the optical wave with the resulting acoustical wave during operation. In this work, we investigate the SBS properties of LMA fibers with confined Ytterbium doping and numerically compare the amplifier performance with homogeneously doped large mode area gain fibers and the corresponding high-power single frequency SBS thresholds.

Keywords: confined doping, fiber laser, single frequency, SBS, directed energy, specialty optical fiber

1. INTRODUCTION

Single frequency fiber laser amplifier designs are continuously being investigated and improved upon for the simultaneous benefit of the gravitational wave detection and directed energy communities. Gravitational wave detectors rely on the extremely long coherence length of single frequency lasers to perform multi-kilometer long laser interferometric measurements in order to detect the slight gravitational distortions due to celestial bodies many light years away.[1] The directed energy community interests are just as sophisticated but the application area is much different. Narrow linewidth lasers are required in the directed energy community for the purpose of investigating and operating high average power beam combinable defense oriented laser systems. With national security goals to build electric lasers beyond 100kW class,[2] the ability to combine many high-performance multi-kW lasers into a single effective output is critical. Spectral linewidths less than 20GHz are commonly desired for both spectral and coherent combining methodologies,[3,4] where even narrower linewidths allow for larger engineering tolerances in the beam combining system design space.

Large mode area (LMA) step index fibers with large core diameters and small numerical apertures (NAs) are essential for the development of kW class fiber lasers with near diffraction limited beam quality.[3] The LMA concept mitigates intensity driven nonlinear effects by distributing the intensity across the cross section of the larger core, thus mitigating power limiting nonlinear effects such as stimulated Brillouin scattering (SBS) and stimulated Raman scattering (SRS). Mode area scaling while preserving single mode guidance is challenging in step index waveguides as the core NA cannot be chosen to be arbitrarily small and the number of supported modes increases as the core becomes larger. Therefore, it is common practice to use few mode LMA fibers for both high power fiber laser oscillators and amplifiers. With respect to single frequency fiber laser amplifier development, recent accomplishments have been mostly derived from custom fabricated large mode area active gain fibers. Pulford et al. achieved a 400W single frequency result at 1064nm in 2015 using an all-solid photonic bandgap fiber with a $50\mu m$ core[5] comprised of many $6.5\mu m$ diameter microstructures. In 2019 Wellmann et al.

Further author information: (Send correspondence to M.A.C)
M.A.C.: E-mail: matthew.cooper@ucf.edu, Telephone: 1 717 474 4001

used a 3m piece of standard step-index Nufern $25/400\mu m$ polarization-maintaining (PM) fiber to attain a 200W single frequency result at 1064nm.[6] In 2020, Dixneuf et al. completed a 365W single frequency experiment by using a custom fiber with a mode field diameter of $34\mu m$ and an NA of 0.055.[7] Most recently, Lai et al. used a tapered Yb-doped LMA fiber 1.27m in length to achieve 500W single frequency at 1030nm.[8]

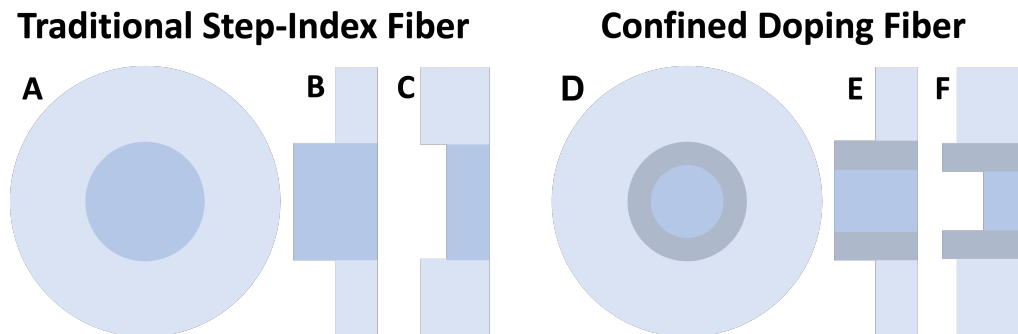## Traditional Step-Index Fiber   Confined Doping Fiber

Figure 1: A notional step-index fiber illustrated in (A) with the corresponding refractive index profile in (B) and the acoustic index profile in (C). A notional confined doping fiber illustrated in (D) with the corresponding refractive index profile in (E) and the acoustic index profile in (F).

One interesting strategy in designing LMA fibers for single mode operation includes exploiting differential propagation losses between the fundamental mode and Higher Order Modes (HOMs). More recent studies revealed that effective higher order mode suppression due to differential gain is possible. Moving away from a homogeneously doped core, the differential gain can be accomplished by modal gain filtering by what is called the confined doping or gain tailoring approach.[9, 10] Here the rare earth doping of the core is limited to the central part of the refractive index matched fiber core. This approach has only been recently studied qualitatively.[11–15] A simple comparison between a step-index and confined-doping fiber is illustrated in Fig. 1.

2. THEORY AND EXPERIMENTAL DESIGN

In this work, we investigate the acoustical guiding properties of a confined doping fiber. Figs. 2a and 2b present an example of two LMA fibers with an identical core diameter of 25μm and a numerical aperture of 0.048. While the core of the first fiber in Fig. 2a is a step-index fiber and is assumed to be homogeneously doped with Ytterbium and Aluminum, the rare earth dopant in the core of the second fiber in Fig. 2b is surrounded by a ring of Germanium doped silica.

(a) SEM image of CREOL made 25/400 μm gain fiber   (b) SEM image of the 25/400 μm CDF under test

Figure 2: SEM images (taken with Phantom ProX by Thermo Fisher Scientific) of the core regions of a the step-index CREOL $25/400\mu m$ gain fiber in (a) and of the confined doping fiber under investigation in (b).

During the fabrication process, this Ge ring is fabricated by surrounding the active core with Germanium doped rods. The doping concentration of this Germanium doped ring in the core of the CDF is chosen to match

the refractive index of the Al-Yb doped silica section of the core so that the optical properties of both fibers are identical as seen in the 2D refractive index profiles (RIPs) in Figs. 3a and 3b.
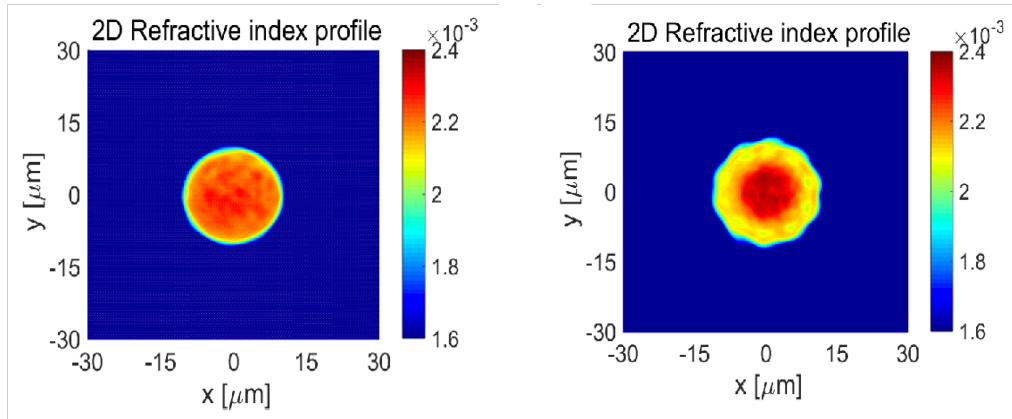

(a) 2D RIP of Step-Index Fiber   (b) 2D RIP of Confined Doping Fiber

Figure 3: 2D Refractive index profiles (measured with IFA-100 by Interfiber Analysis) of step index $25/400\mu m$ gain fiber in (a) and of the confined doping fiber under investigation in (b).

A more detailed side-by-side comparison of both the optical and acoustical index profiles are illustrated in Fig. 4 of idealized fibers based on the index changes due to dopant materials in the host glass. The optical refractive index is outlined in black whereas the acoustical index profile is outlined in red. In the step index fiber, the acoustical profile is an inverted version of the optical profile. In the CDF the Ge components of the core add a high acoustical index near the core but do not effect the optical index profile.
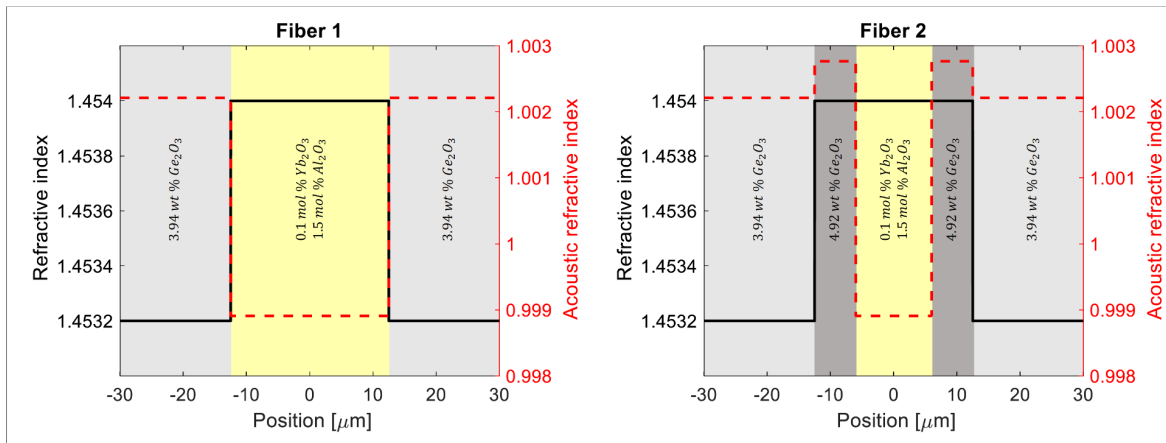
(a) Step Index Fiber Profiles   (b) Confined Doping Fiber Profiles

Figure 4: Idealized optical refractive index, acoustic refractive index, and doping profile of a fiber with homogeneously contributed rare earth dopant distribution in the core region (a) and a confined rare earth rare earth dopant distribution in the core region (b).

The evolution of the complex overlap (γ_{ao}) between the optical and the acoustic waves that propagate without material damping in the acoustic refractive index landscape of Fiber 1 and Fiber 2 is illustrated in Fig. 5. Furthermore, the material damping of acoustic waves that propagate in bulk silica doped with 1.5 mol% Al_2O_3 and 0.1 mol% Yb_2O_3 and 3.94 wt% Ge_2O_3 is illustrated in Figs. 5(A) and 5(C) for comparison. The material damping coefficients used to calculate the acoustic damping in these estimates have been calculated with the adaptive model for binary and trinary glasses and the material constants from Ballato et al.[16] The evolution of the acoustic wave, which has been excited by the optical fundamental mode, in the acoustic refractive index
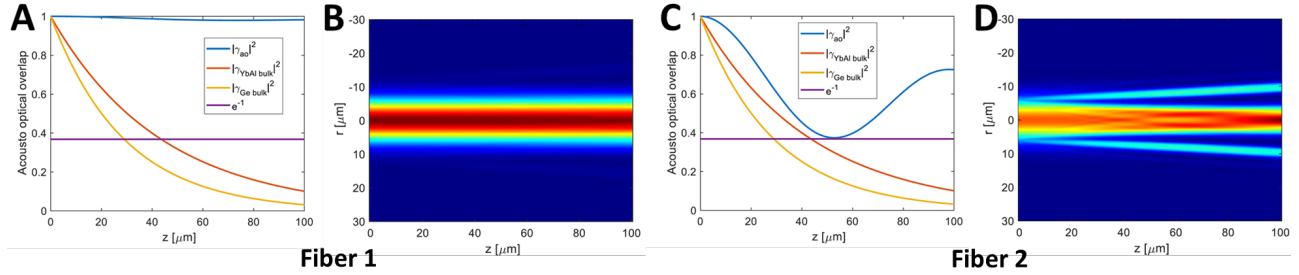
Fiber 1   **Fiber 2**

Figure 5: Evolution of the transverse amplitude distribution of electrostinctively excited acoustic density wave propagating in a fiber with a homogenous rare earth dopant distribution in the core region (Fiber 1) and a confined rare earth rare earth dopant distribution in the core region (Fiber 2).

of fiber 1 and fiber 2 has been calculated from an acoustic BPM and is illustrated in the adjacent Figs. 5(B) and 5(D). The acousto-optical overlap of Fiber 1 gives no significant change at the length scale of the acoustic material absorption on the order of $100\mu m$ shown in blue in Fig. 5(A), whereas the overlap within Fiber 2 in Fig. 5(C) drops significantly within the same distance scale. This leads to the effective broadening of the Brillouin gain linewidth[17] resulting in what appears to be a more 'dispersed' acoustic wave as seen in Fig. 5(D) as opposed to the continuous acoustic beam propagation of the step index fiber in 5(B).
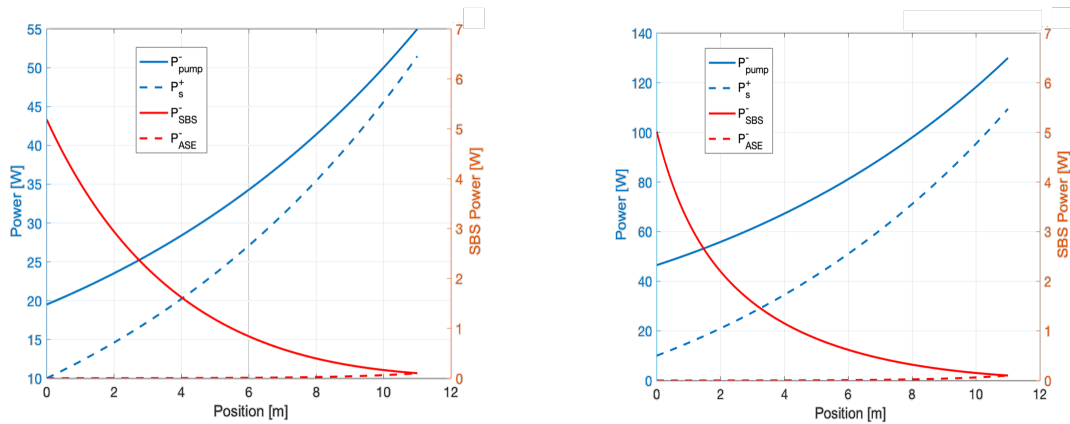
(a) Estimated amplifier results from Fiber 1   (b) Estimated amplifier results from the CFD

Figure 6: Estimated fiber laser amplifier performance with respect to output signal power (dashed blue line), and the reflected SBS response (solid red line) with a pump power absorption (solid blue line) along an 11m piece of gain fiber.

In order to illustrate the expected change in SBS threshold between both fibers we modeled two counter pumped fiber laser amplifiers following[18] as shown in Figs. 6b and 6a. Seeded with 5W at $1030\mu m$ and pumped at $976\mu m$ assuming a cladding size needed to absorb 90% of the pump light for a fiber length of 11m. Fig. 6b shows the amplifier pump power in blue, the seeded signal power in the dashed blue line, the reflected SBS in red, and ASE in dashed red. For the step index fiber an arbitrary pump power level of 55W is chosen as the initial point of comparison. When applying the confined doping core into the models, a pump power level of 130W is achieved in order to give rise to an identical level of reflected SBS signal. A 2.4x enhancement of peak output power due to an increase in SBS threshold is numerically modeled thus an improvement should be easily measured experimentally.

The experimental setup is illustrated in Fig. 7. The seed source consists of a two single mode fiber amplification stage and a temperature controlled Yb-crystal single frequency seed laser with less than 10kHz linewidth. The average power of the single frequency seed laser reached up to 40W but only a seed power of 5W has been used for the experiment as this was sufficient to saturate the LMA amplifier. The linearly polarized single
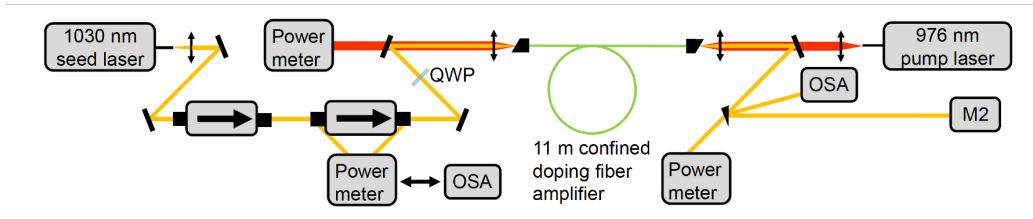
Figure 7: Schematic of the third single frequency laser amplification stage utilizing 11m of confined doping fiber, the first two stages are incorporated in the pre-amplifier within the 1030nm seed source block.

frequency source is free spaced coupled through two 30dB isolators and a quarter wave plate (QWP) into the third amplification stage with the fiber under test. The QWP is used to convert the linearly polarized input into circularly polarized light. Two angled (2.5 degrees) and antireflection coated end caps are used to minimize Fresnel reflections at the glass/air interface of the active fiber. The gain fiber itself is coiled around a 40cm diameter mandrel and water cooled at 19C. The 976nm pump light from an Optical Engines laser is delivered by a 220/240µm and 0.22NA fiber and free spaced coupled into the gain fiber through a dichroic mirror and via a 1:1 telescope. The dichroic mirror reflects the output signal light to the output diagnostics and prevents any signal light from coupling back into the pump sources. An M^2 system, an optical spectrum analyzer, and a Gentec-EO beam profiler are monitoring the output's performance.

3. FINAL EXPERIMENTAL AND RESULTS

A single-frequency output of 123.1W is achieved and a polarization extinction ratio (PER) of 20dB is measured on the output. The output beam profile is recorded and displayed in Fig. 8(a) showing a 4-sigma M^2 of 1.11. Additionally, the output spectrum at the initial seed power and final output power is presented in Fig. 8(b) showing that the $25/400µm$ confined doping fiber based amplifier has maintained more than 37dB of separation from the ASE noise floor.

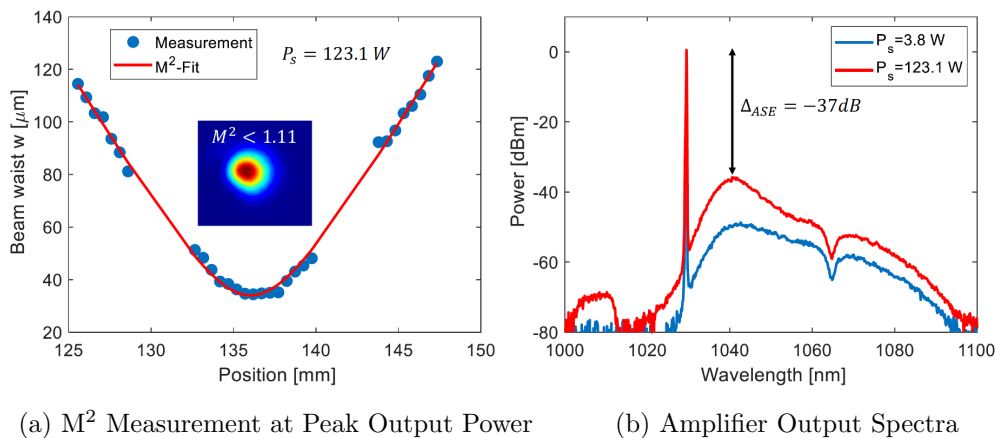(a) M² Measurement at Peak Output Power   (b) Amplifier Output Spectra

Figure 8: M² measurements and beam profile inset of the amplified signal exciting the confined doping fiber amplifier (a). Measured output spectrum at 3.8 W and 123.1 W signal power in (b). Both spectra have been measured with a resolution setting of 0.02 nm and a sensitivity setting of "High 2"

The measured forward and backward power are shown in Figs. 9(a) and 9(b). A slope efficiency is calculated to be 92% based on the absorbed pump power and the signal power out. The reflected power in red show a steadily increasing trend as the power increases, just as one would expect, until reaching 100W then the reflected power begins to shoot up rapidly indicating the tell-tale spike due to SBS in single-frequency fiber lasers. At the

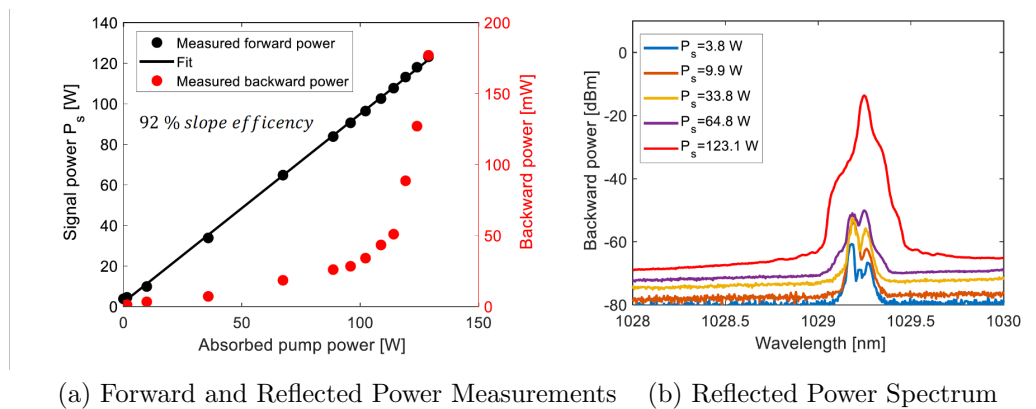(a) Forward and Reflected Power Measurements   (b) Reflected Power Spectrum

Figure 9: Signal output power after the second amplification stage and reflectivity as a function of launched pump power are shown in (a). Measured backward spectra at various amplifier output power levels in (b). All spectra have been measured with a resolution setting of 0.02 nm and a sensitivity setting of "High 2".

peak power in this experiment of 123W the amplifier was experiencing too much backward power fluctuations and the risk to the seed laser was too great to continue increasing the pump power.

4. CONCLUSION

In summary, this research highlights the benefits of using confined-doping fibers to increase the SBS threshold in fiber laser amplifiers. We have demonstrated a 123W single frequency fiber laser amplifier at 1030nm via an 11m 25/400 μm confined doping, also known as gain tailored, double-clad active gain Yb-doped fiber. A near diffraction-limited output is achieved with an M^2 of 1.11, an extremely high slope efficiency of nearly 92% which is close to the quantum defect limit, and a PER of 20 dB. This is more than a two times enhancement in output power over an equivalent single frequency fiber laser amplifier based on a homogeneously doped 25/400 μm double clad step-index fiber.

REFERENCES

[1] Abramovici, A., Althouse, W. E., Drever, R. W. P., Gürsel, Y., Kawamura, S., Raab, F. J., Shoemaker, D., Sievers, L., Spero, R. E., Thorne, K. S., Vogt, R. E., Weiss, R., Whitcomb, S. E., and Zucker, M. E., "Ligo: The laser interferometer gravitational-wave observatory," *Science* **256**(5055), 325–333 (1992).

[2] Sayler, K. M., Feickert, A., Hoehn, J. R., and O'Rourke, R., "Department of defense directed energy weapons: Background and issues for congress," Tech. Rep. R46925, Congressional Research Service (2021). https://crsreports.congress.gov.

[3] Anderson, B. M., MacDonald, K., Taliaferro, A., and Flores, A., "SBS suppression techniques in high-power, narrow-linewidth fiber amplifiers," in [*Fiber Lasers XVIII: Technology and Systems*], Zervas, M. N., ed., **11665**, 63 – 69, International Society for Optics and Photonics, SPIE (2021).

[4] Wellmann, F., Bode, N., Wessels, P., Overmeyer, L., Neumann, J., Willke, B., and Kracht, D., "Low noise 400 w coherently combined single frequency laser beam for next generation gravitational wave detectors," *Opt. Express* **29**, 10140–10149 (Mar 2021).

[5] Pulford, B., Ehrenreich, T., Holten, R., Kong, F., Hawkins, T. W., Dong, L., and Dajani, I., "400-w near diffraction-limited single-frequency all-solid photonic bandgap fiber amplifier," *Opt. Lett.* **40**, 2297–2300 (May 2015).

[6] Wellmann, F., Steinke, M., Meylahn, F., Bode, N., Willke, B., Overmeyer, L., Neumann, J., and Kracht, D., "High power, single-frequency, monolithic fiber amplifier for the next generation of gravitational wave detectors," *Opt. Express* **27**, 28523–28533 (Sep 2019).

[7] Dixneuf, C., Guiraud, G., Bardin, Y.-V., Rosa, Q., Goeppner, M., Hilico, A., Pierre, C., Boullet, J., Traynor, N., and Santarelli, G., "Ultra-low intensity noise, all fiber 365 w linearly polarized single frequency laser at 1064 nm," *Opt. Express* **28**, 10960–10969 (Apr 2020).

[8] Lai, W., Ma, P., Liu, W., Huang, L., Li, C., Ma, Y., and Zhou, P., "550 w single frequency fiber amplifiers emitting at 1030nm based on a tapered yb-doped fiber," *Opt. Express* **28**, 20908–20919 (Jul 2020).

[9] Mermelstein, M. D., "Sbs threshold measurements and acoustic beam propagation modeling in guiding and anti-guiding single mode optical fibers," *Opt. Express* **17**, 16225–16237 (Aug 2009).

[10] Robin, C., *Novel approaches to power scaling of single-frequency photonic crystal fiber amplifiers*, PhD thesis, The University of New Mexico (2011).

[11] Seah, C. P., Lim, W. Y. W., and Chua, S.-L., "A 4kw fiber amplifier with good beam quality employing confined-doped gain fiber," in [*Laser Congress 2018 (ASSL)*], *Laser Congress 2018 (ASSL)* **1**, AM2A.2, Optical Society of America (2018).

[12] Liao, L., Zhang, F., He, X., Chen, Y., Wang, Y., Li, H., Peng, J., Yang, L., Dai, N., and Li, J., "Confined-doped fiber for effective mode control fabricated by mcvd process," *Appl. Opt.* **57**, 3244–3249 (Apr 2018).

[13] Gausmann, S., Lopez, J. E. A., Anderson, J., Wittek, S., Correa, R. A., and Schülzgen, A., "Gain dependent mode analysis of large mode area fiber with confined ytterbium doping," in [*Conference on Lasers and Electro-Optics*], *Conference on Lasers and Electro-Optics* **1**, SM4L.3, Optical Society of America (2019).

[14] Zhang, F., Wang, Y., Lin, X., Cheng, Y., Zhang, Z., Liu, Y., Liao, L., Xing, Y., Yang, L., Dai, N., Li, H., and Li, J., "Gain-tailored yb/ce codoped aluminosilicate fiber for laser stability improvement at high output power," *Opt. Express* **27**, 20824–20836 (Jul 2019).

[15] Gausmann, S., Antonio-Lopez, J. E., Anderson, J., Wittek, S., Eznaveh, S. E., Jang, H.-J., Habib, M. S., Cook, J., Richardson, M. C., Correa, R. A., and Schülzgen, A., "S^2 measurements showing suppression of higher order modes in confined rare earth doped large core fibers," *Journal of Lightwave Technology* **38**(7), 1953–1958 (2020).

[16] Ballato, J., "Rethinking optical fiber: New demands, old glasses," in [*Workshop on Specialty Optical Fibers and their Applications*], *Workshop on Specialty Optical Fibers and their Applications* **1**, W1.1, Optical Society of America (2013).

[17] Dragic, P. D., Liu, C.-H., Papen, G. C., and Galvanauskas, A., "Optical fiber with an acoustic guiding layer for stimulated brillouin scattering suppression," in [*Conference on Lasers and Electro-Optics/Quantum Electronics and Laser Science and Photonic Applications Systems Technologies*], *Conference on Lasers and Electro-Optics/Quantum Electronics and Laser Science and Photonic Applications Systems Technologies* **1**, CThZ3, Optical Society of America (2005).

[18] Hildebrandt, M., Büsche, S., Weßels, P., Frede, M., and Kracht, D., "Brillouin scattering spectra in high-power singlefrequency ytterbium doped fiber amplifiers," *Optics express* **16**(20), 15970–15979 (2008).